The effect of a magnetic field on the near-surface substructure of domain walls in single-crystal iron

V. E. Zubov, G. S. Krinchik, and S. N. Kuz'menko

M. V. Lomonosov State University at Moscow
(Submitted 19 June 1990)
Zh. Eksp. Teor. Fiz. **99**, 551–561 (February 1991)

We describe the first investigations of magnetization reversal processes in the near-surface substructure of 180° domain walls in filamentary single crystals of iron based on observation of the motion of Bloch points. We have observed the annihilation of pairs of Bloch points in an external magnetic field, and a considerable increase in the coercivity of the various microstructural elements—domain walls, vertical Bloch lines, and Bloch points—with decreasing dimensionality. The coercive field of a Bloch point (H_c^{BP}) also decreases in the presence of domain-wall oscillations; in fields smaller than H_c^{BP} the Bloch points exhibit a relaxation-type spectrum of oscillations activated by domain-wall pumping. For motion over the magnetic barrier ($H > H_c^{BP}$) we observed a considerable increase in the amplitude of oscillation of the Bloch points at frequencies above 100 kHz; this is associated with the decrease in their dynamic coercive field.

1. INTRODUCTION

The exit of a domain wall to the surface of a bulk ferromagnet is a one-dimensional formation with its own special structure and dynamic properties. In Ref. 1 it was experimentally shown for the first time that 180° domain walls in the near-surface region of single crystals of iron have a Néel component of the magnetization (i.e., perpendicular to the domain wall plane) that is close in value to the saturation magnetization I_s.

Recently an analogous result was obtained by the method of spin-polarization microscopy.[2] The structure investigated in Ref. 2, which is shown in the inset to Fig. 1, is closest to the model of a 180° asymmetric Bloch wall proposed by Hubert.[3] Local rearrangement of the domain wall structure sharply decreases the value of the stray fields localized in the vicinity of points where the domain wall exits the surface. The energy of the domain wall does not depend on the direction it bends toward in the near-surface region, i.e., there is degeneracy with respect to the sign of the Néel component of the magnetization. This circumstance implies that the near-surface region of the domain wall will split up into subdomains, i.e., regions with different signs of the Néel component of the magnetization and/or bending directions.

Using the results of our investigation of the magnetization distribution in the region where the domain wall exits the surface, we were able to classify the pointlike singularities that separate the various domain-wall subdomains.[4] We found that there are two types of VBL (vertical Bloch line) exits at the surface. For one of these exits the domain walls on different sides of the VBL bend in the same direction (VBL-1), while for the other they bend in opposite directions (VBL-2). Because the sign of I_z for the domain wall is different on different sides of the VBL deep in the crystal bulk, in the first case the sign of I_x at the surface changes as we pass through the VBL, while in the second case it is unchanged (the coordinate system is shown in Fig. 1). The Bloch-point type of feature is a microstructural element similar to a Bloch line; it separates two subdomains in the one-dimensional near-surface structure with different polarities while leaving the polarization of the domain wall in the bulk unchanged. Furthermore, as we move along a domain wall and pass through a VBL, when the latter is of VBL-1 type there is no lateral displacement of the domain wall at the surface, while for the VBL-2 type there is a displacement of ~4 Å; this is also true for the case of a Bloch point. The structures of a VBL-1 and a Bloch point are shown in Fig. 1, while a VBL-2 structure is shown in Fig. 2b.

In this paper we investigate how Bloch points and VBL exits are distributed in the near-surface region of a 180° domain wall within a filamentary single crystal of iron, the most perfect type of iron crystal known today. We study static and quasistatic magnetization reversal processes for domain walls due to motion of VBL's, and similar processes in the near-surface region of a domain wall due to motion of Bloch points, and describe our measurements of the coercive fields of domain walls, VBL's, and Bloch points in the same crystal. We will study the processes of Bloch point motion in AC magnetic fields with frequencies up to 1 MHz, and describe our observations of the relaxation spectrum of Bloch point oscillations in fields below the coercive field.

2. METHODS OF MEASUREMENT AND SAMPLES

In our experimental investigation we used a phase-sensitive magneto-optic micromagnetometer with a working frequency range of 20 Hz to 30 MHz, as described in Ref. 4. In this paper the measurement part of the setup was designed with the intent to broaden the frequency range down to a frequency of 0.5 Hz. For this we used differential switching of a photomultiplier combined with a low-frequency phase detector. In order to measure the components of the magnetization lying in the magnetic mirror plane, we used the magneto-optic equatorial Kerr effect (EKE) and meridional Kerr effect (MKE).

In this work we studied filamentary iron crystals obtained by hydrogen reduction of iron halide salts according to the method described in Ref. 5. By varying parameters such as growth temperature, hydrogen flux rate, and boat material and quantity of the original salt, we obtained crys-

 0038-5646/91/020307-07$03.00

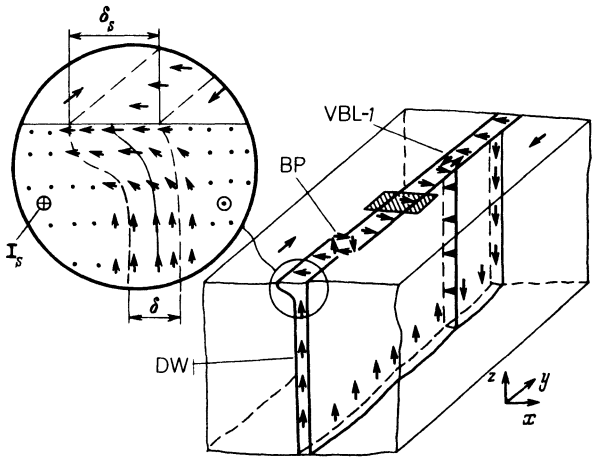

FIG. 1. Sketch for a segment of 180° domain wall containing VBL's and Bloch points (BP). In the inset we show the model of an asymmetric 180° domain wall postulated by Hubert;[3] δ is the effective width of the domain wall in the bulk, and δ_s its width at the surface.

tals of various sizes and shapes. For our measurements we chose samples of square cross-section with sides $d = 30$ to 150 μm and lengths $L = 2$ to 10 mm with natural optically perfect (100) facets. The domain structure of the samples was made visible using the MKE in a setup assembled at the base of an MBS-10 microscope. The investigation was carried out on samples containing one 180° domain wall located in the center along the crystal axes and parallel to the lateral facets. In order to investigate the domain wall structure on various facets of the sample, we glued a cover glass of thickness 150 μm onto the butt-end portion of the sample. By rotating this glass in a special setup, we were able to study

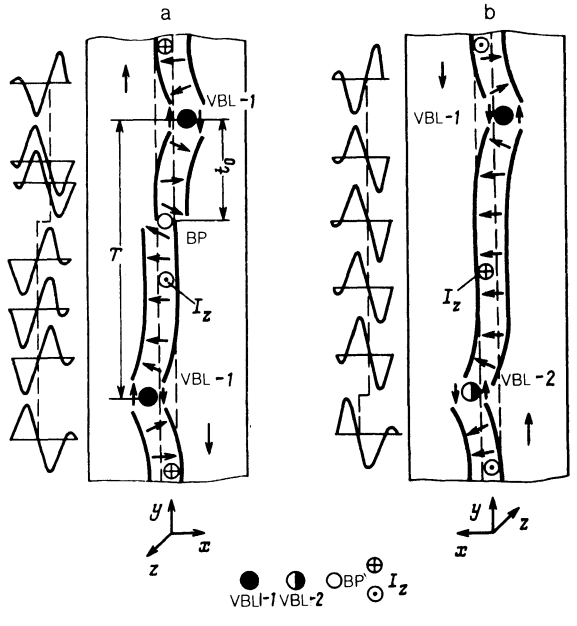

FIG. 2. Exit structures on two opposite facets of a crystal (a and b) for a section of domain wall. The position of the domain wall in the bulk is shown by dashed lines; I_z is the direction of the magnetization in the bulk of the domain wall. To the left near the sketches of the crystal facets we show EKE curves caused by the Néel components of the magnetization for the corresponding segments of the domain wall.

the three facets of the crystal in turn using an immersion objective.

The fields H_x and H_z were precisely oriented relative to the crystal axes (see Fig. 1) by mounting the sample on an alignment microscope stage. The field orientation relative to the longitudinal axis of the crystal was controlled by measuring the MKE associated with oscillations of the domain wall. These oscillations appear when the fields H_x or H_z have nonzero projections in the direction of the domain magnetization. As the signs of these projections vary the MKE also changes sign. By rotating the sample in H_x or H_z fields with sufficiently large amplitudes (~ 100 Oe), we succeeded in reducing the MKE to zero, thereby establishing that these fields were perpendicular to the magnetization vector within the domains to an accuracy of several thousandths of a degree.

3. NEAR-SURFACE SUBSTRUCTURE OF A DOMAIN WALL

The substructure was revealed by magnetooptic methods; specifically, the EKE was used to determine the direction of bend of the domain wall and the sign of the Néel component of the magnetization at various points along the domain wall. The measurements were carried out while the domain wall was oscillating with an amplitude $\Delta_{D\omega} \sim \delta$ (where $\delta \sim 0.2$ μm; see Fig. 1) under the action of an AC magnetic field H_y. In this case EKE curves due to the Néel component of the magnetization in the domain wall exhibit sign changes. Possible variants of such curves are shown in Fig. 2. The order of alternation of the primary maxima and minima is determined by the sign of the Néel component. The direction of bend of the boundary can be determined according to the position of the small extremum relative to the two primary ones. Specifically, the domain wall bends toward the side opposite that on which the small extremum is located.[4] The sign of the Néel component can be determined independently based on the direction of motion of a Bloch point in the constant field H_x. The direction of the magnetization in the domains and the subdomains of the boundary within the sample is determined from the sign of domain-wall motion in the field H_y and the sign of VBL motion in the field H_z respectively.

Figure 2 shows the near-surface structure of two ends of a single portion of the domain wall on opposite facets of the crystal. The basic parameters that characterize the substructure are the distance between adjacent VBL (T) and the distance between a Bloch point and the VBL closest to it (t_0); it is found that T increases as the sample thickness increases. The substructure is only quasiperiodic, because there is a scatter in values of T along the domain wall. The magnitude of the fluctuations in T decreases as the thickness of the sample decreases. The pattern most often encountered in the domain wall is a segment of the form VBL-Bloch point-VBL, as illustrated in Fig. 2a. Sequences of this kind can be interrupted by one or several segments of the form VBL–VBL (Fig. 2b); the VBL-2 is encountered more rarely than the VBL-1.

It is clear from Fig. 2 that the domain wall has a zig-zag form. Bending of the boundary is observed only in regions adjacent to the VBL. The angle of this bending has a value 1.5° to 3°, and decreases by a factor of 2 to 3 over a distance of ~ 20 Å from the VBL. The signs of the bend angles are dif-

ferent for successive VBL. Furthermore, bending angles have different signs on opposite facets of the crystal at the ends of the same VBL (see Fig. 2). According to the calculations of Shtrikman and Trevers,[6] the bending is localized in the near-surface region, and its appearance enables the magnetic flux to close in adjacent subdomains of a domain wall separated by a VBL.

As a rule the Bloch points occupy asymmetric positions between the VBL's. This is associated with the presence of a stray field (H_{str}) arising from a rather small nonparallel orientation of opposite facets of the crystal and having a component along the x axis ($H_{str,x}$). For the samples we investigated the angle of deviation from parallelism between facets varied; the maximum value of this angle came to $\sim 0.3°$. For such small angles we can use the estimate $H_{str,x} \lesssim 150$ Oe for the value of the field H_x at positions along near-surface segments of the domain wall.

4. MOTION OF A BLOCH POINT IN A CONSTANT MAGNETIC FIELD

It is clear from Figs. 1 and 2 that a Bloch point divides two subdomains with different signs of the Néel component of magnetization and directions of domain-wall bending. In a field H_x the degeneracy of the subdomain with respect to energy is lifted, which causes the Bloch points to move. Figure 3 show how the distance t between a Bloch point and one of the VBL depends on the value of the constant magnetic field H_x (here and in what follows we will assume that the fields H_x and H_z arise from external sources, i.e., we will ignore the demagnetizing fields of the samples). The position of the Bloch point was determined using the method described in the previous section. Curve *1* characterizes the position of a Bloch point within a subdomain with parameters $T = 165\ \mu$m, $t_0 = 25\ \mu$m, while curve *2* corresponds to parameters $T = 80\ \mu$m, $t_0 = 18\ \mu$m.

The differential susceptibility of a near-surface segment of the domain wall between two VBL caused by VBL motion is determined by the coefficient $K_x^{BP} = \partial t(H_x)/\partial H_x$. On the linear portion of curve *1* the value of K_x^{BP} comes to $2\ \mu$m/Oe, while for curve *2* it is $0.8\ \mu$m/Oe. The nonlinear portion of these curves begins when the distance between the Bloch point and VBL equals $\sim 25\ \mu$m; this is the distance at which bending of the domain wall becomes appreciable. The Bloch point approaches the VBL (i.e., t decreases) monotonically up to fields $H_x \sim 400$ Oe, at which point the distance between the two features has decreased to a value of $\sim 1\ \mu$m. For larger values of the field there is a discontinuous change in the near-surface domain wall structure: the boundary widens and the magnetization vector in the near-surface region of one of the domains orients itself parallel to the field H_x.

In the previous section we explained the asymmetric position of the Bloch point for $H_x = 0$ as an effect of stray fields that appear because of deviations from parallelism of opposite facets of the crystal. Using the curves $t(H_x)$ shown in Fig. 3, we can estimate the value of the field $H_{str,x}$ in the near-surface region of the domain wall. By virtue of the equivalence of the VBL on the two sides of the Bloch point, in the absence of a field parallel to the x axis a Bloch point should be found at equal distances from neighboring VBL. Consequently, if a Bloch point is located symmetrically relative to a pair of VBL, then $H_x + H_{str,x} = 0$. It is clear from Fig. 3 that for both the cases shown the value of $H_{str,x}$ is ~ 20 Oe. The angle between the near-surface facets of the crystal at which curves *1* and *2* in Fig. 3 were measured came to $\sim 0.05°$, which agrees with the estimates made in Sec. 3.

During magnetization reversal of the domain wall in AC fields H_x and H_z with amplitudes ~ 500 Oe, groups of several Bloch points sometimes appeared located between adjacent VBL's; this allowed us to study how Bloch point pairs approach one another under the action of a constant field. In Fig. 4 we show a curve that describes how two Bloch points approach and annihilate each other as the field H_x increases. A schematic illustration of such a pair of points is shown in the inset to Fig. 4. In the absence of a field H_x the distance between Bloch points (t_{12}) comes to $45\ \mu$m. The quantity t_{12} varies almost linearly with field up to the value $H_x \sim 100$ Oe. At this point the distance between the points has decreased to $t_{12} \approx 5\ \mu$m. Beyond this point the two points approach each other more slowly as the field increases. For $H_x \approx 150$ Oe the value of t_{12} is between 0.3 and $0.5\ \mu$m; in a field of 170 Oe the two Bloch points annihilate.

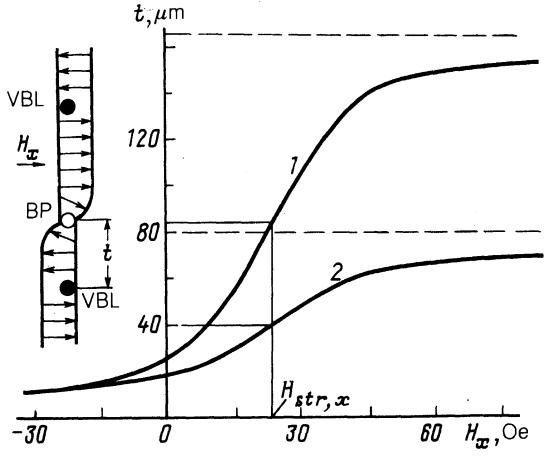

FIG. 3. Dependence of the distance between a VBL and a moving Bloch point on the constant magnetic field H_x when the Bloch point is located between two VBL's. The coordinate origin was chosen at one VBL, while the position of the other is denoted by the dashed lines. Curve *1* corresponds to a subdomain with $T = 165\ \mu$m, curve *2* to a subdomain with $T = 80\ \mu$m.

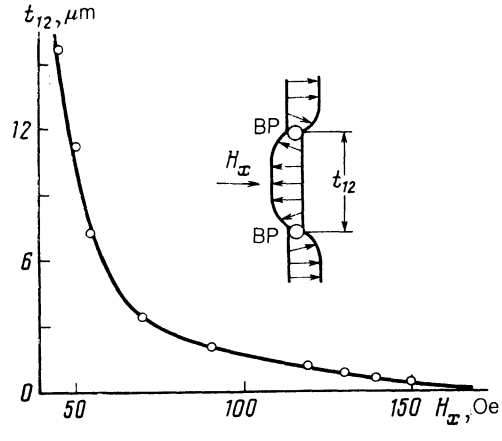

FIG. 4. Dependence of the distance t_{12} between two Bloch points on the constant field H_x.

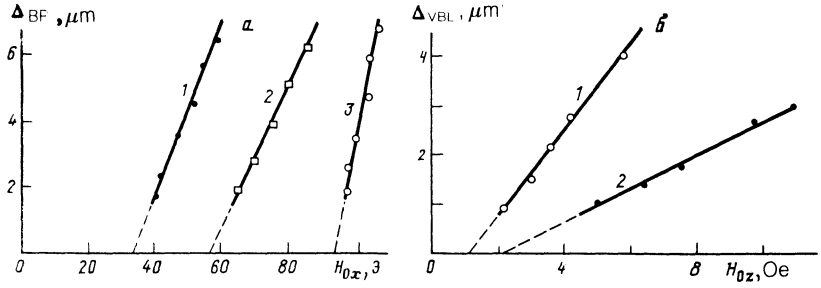

FIG. 5. Characteristic dependence of the amplitude of oscillations for several Bloch points (a) and VBL's (b) for various values of H_c on the amplitudes of the fields H_x and H_z; the frequency of the fields H_x and H_z. were 60 Hz. The values of the coercive fields were: (a)—H_c^{BP} = 34 Oe (*1*), 57 Oe (*2*), 93 Oe (*3*); (b)—H_c^{VBL} = 1.2 Oe (*1*), 2.1 Oe (*2*).

5. COERCIVITIES OF BLOCH POINTS, VBL'S AND DOMAIN WALLS

We studied the motion of Bloch points in AC fields in the following way. When the input window of the photodetector was moved parallel to the domain wall along the y axis, a magneto-optic signal was observed only from that segment of the domain wall whose magnetization was reversed due to Bloch-point oscillations under the action of the AC field H_x. Our photometric measurements were made on local rectangular sections of the sample surface with dimensions $0.2\times2\,\mu m^2$, with the long side of the rectangle perpendicular to the domain wall (the dashed region in Fig. 1). We measured EKE curves caused by the Néel component of the magnetization in the domain wall. The width of the EKE curves obtained in this way allowed us to determine how the oscillation amplitude of the Bloch point (Δ_{BP}) depended on the field amplitude (H_{0x}).

Figure 5a shows characteristic examples of the function $\Delta_{BP}(H_{0x})$ derived from studies similar to those described in Ref. 7. From Fig. 5a it is clear that the experimental points lie quite close to a straight line; the tangent of the slope angle of this line determines the value of the coefficient $K_x^{BP} = 0.4$ μm/Oe. Extrapolating the line $\Delta_{BP}(H_{0x})$ to the value $\Delta_{BP} = 0$ allows us to determine H_c^{BP}, i.e., the value of the Bloch-point coercive field, analogous to the method used for a domain wall.[8] For all the points investigated, the value of the field H_c^{BP} lay within the interval 30 to 100 Oe. Another method for determining the value of H_c^{BP} is to measure the phase shift (φ) of the Bloch-point oscillations relative to the field H_x due to the coercivity of the Bloch point and determined by the relation $\varphi \approx \arcsin(H_c^{BP}/H_{0x})$. The value of H_c^{BP} obtained using this method is in good agreement with the results of measuring the function $\Delta_{BP}(H_{0x})$.

For purposes of comparison we carried out an investigation of the processes of VBL and domain-wall motion in an AC magnetic field in the same sample. The coefficient K_z^{VBL} characterizes the susceptibility of a domain wall in the course of VBL motion in the field H_z; the value of this coefficient increases as the thickness of the sample is increased, and the period of the substructure T also varies within the limits 0.1 to 1 μm/Oe. Typical dependences $\Delta_{VBL}(H_{0z})$ are shown in Fig. 5b, where H_{0z} is the amplitude of the field H_z. The values of H_c^{VBL} for curves *1* and *2* equaled 1.2 Oe and 2.1 Oe respectively. The same values were obtained by computing H_c^{VBL} using the results of measuring the phase shift for VBL oscillations relative to the field H_z using the relation $\varphi \approx \arcsin(H_c^{VBL}/H_{0z})$. For the VBL investigated here the measured field H_c^{VBL} was found to lie within the limits 1 to 3 Oe.

In order to estimate the value of H_c^{DW} we measured the function $\Delta_{DW}(H_{0y})$ over a wide range of variation of the amplitude (H_{0y}) of the field H_y. It is necessary to distinguish three regions of values for Δ_{DW}, for each of which our method of measuring Δ_{DW} had its own peculiarities: (1) $\Delta_{DW} > \delta_s$, (2) $\Delta_{DW} \sim \delta_s$, and (3) $\Delta_{DW} < \delta_s$. In the first and third cases the input window of the photodetector, which had dimensions $0.2\times3.5\,\mu m^2$, was oriented with the long side parallel to the domain wall, while in the second case this side was perpendicular to the wall (see the insets a and b for Fig. 6). In the first case Δ_{DW} was determined from the width of the EKE curves due to variation of the magnetization component I_y as the domain wall oscillates (for more detail on this see Ref. 4). In the third region the EKE is proportional to the quantity $[\partial I_y(x)/\partial x]\cdot\Delta_{DW}$ (see Ref. 4), where $I_y(x)$ is the distribution of the component I_y in the domain wall; in this case Δ_{DW} can be measured in arbitrary units. In order to join the results obtained in the first and third cases we carried out measurements using the geometry shown in inset b to Fig. 6. If the domain wall does not go outside the bounds of the photodetector window during its oscillations, i.e., $2\Delta_{DW} < 3.5\,\mu$m, then the value of the EKE is proportional to Δ_{DW}. The measurements unambiguously show overlap of the ranges of variation of Δ_{DW} for the first case (indicated by crosses in Fig. 6) and second case (indicated by empty circles), as well as for the second case and

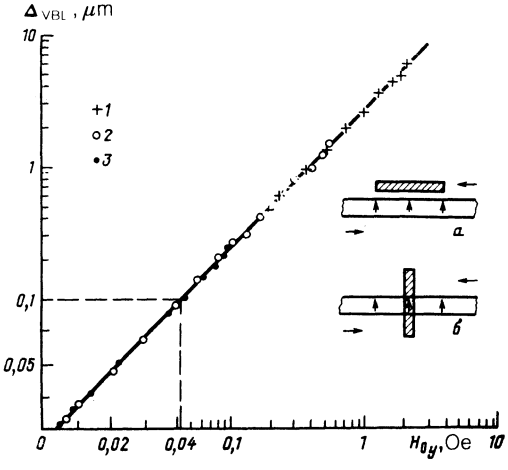

FIG. 6. Dependence of the amplitude of oscillation of a domain wall on the amplitude H_{0y} of the field H_y. The frequency of the field H_y was 60 Hz. Points *1* and *3* are for parallel orientation of the photodetector slot and the domain wall (see inset a), while point *2* is when the two are mutually perpendicular in orientation (inset b).

third case (indicated by black circles). Therefore we have established that Δ_{DW} depends linearly on H_{0y} as the amplitude of this field varies over three orders of magnitude. The minimum measured value of Δ_{DW} came to ~ 30 Å.

The quantity H_c^{DW} was determined by the length of the segment along the abscissa from the coordinate origin to the point where the line $\Delta_{DW}(H_{0y})$ intersects this axis. It is clear from Fig. 6 that the value of H_c^{DW} is less than 0.01 Oe. We observed no phase shift of the domain wall oscillations relative to the field H_y until $H_{0y} = 0.01$ Oe. Estimates of the value of H_c^{DW} obtained by measuring the phase relations for domain wall oscillations and using the expression $\varphi \approx \arcsin(H_c^{DW}/H_{0y})$ agree with what was presented above. Therefore in going from a domain wall to a VBL the coercive field increases by two to three orders of magnitude, while in going from a VBL to a Bloch point it increases by more than an order of magnitude.

Measurements of Δ_{DW} made at various points along various segments of the boundary show that the oscillations of the domain wall are uniform. These oscillations were monitored over segments of the domain wall of lengths 1 to 3 mm at intervals of 10 to 50 μm. For the crystals under investigation estimates for H_c^{DW} coincided with what was presented above along the entire boundary. We also measured H_c^{BP} and H_c^{VBL} for the motion of a Bloch point and a VBL along the domain wall over distances up to several tens of microns at various points on the wall by using constant fields H_x and H_z respectively. Motion of the Bloch point and the VBL did not lead to a change in their coercive fields. The amplitude of oscillations of the Bloch point and VBL depended linearly on the field for values of Δ_{BP} and Δ_{VBL} from a few μm down to values of less than 1 μm, whereas for the case of a domain wall the linear dependence of Δ_{DW} on H_{0y} was observed over a range of variations of Δ_{DW} from 10 μm down to 30 Å.

This data allows us to conclude that the coercive fields in our samples are due to point defects with dimensions smaller than the characteristic dimensions of the structures under discussion ($\delta \approx 0.2$ μm is the width of a domain wall in the bulk). This conclusion is consistent with the well-known fact that filamentary crystals, in particular iron crystals, possess crystallographic and magnetic structures with very high degrees of perfection.[9] According to Ref. 10 the dislocation density in filamentary crystals of iron ranges from 10^4 to 10^5 cm^{-2}, i.e., there is one dislocation per square segment of surface with sides 30 to 100 μm long. This clearly implies that the coercivity of the microstructural elements under discussion here cannot be explained by clamping at dislocations.

We also note the recent work of Heinrich *et al.*,[11] who showed by using the method of fast-electron diffraction that filamentary single crystals of iron have a perfect surface structure characterized by the presence of atomic steps with heights of a few angstroms located at distances larger than several hundred angstroms from one another. From this we may conclude that the coercivities of Bloch points and VBL exits at the surface are essentially caused by the same phenomena that gives rise to the coercivity of domain walls and VBL in the bulk crystal.

The results we have obtained, along with observations of analogous effects for domain walls and VBL in other materials,[8,12] allow us to assert that the observed differences in values of H_c are essentially determined by the dimensionality of the microstructural elements. This conclusion can be illustrated using the following considerations. The value of H_c for a microstructural element is determined by the condition that the pressure on the element due to the external field is equal to the confining force per unit area exerted by the crystal defects, i.e., from the equation $2I_sSH = F_c$, where S is the effective area of the element over which the pressure due to the external field is applied. For the case of point defects F_c is determined[13] by fluctuations in the number N of defects in a volume element V, i.e., $F_c \propto \Delta N \sim (N)^{1/2} = (nV)^{1/2}$, where ΔN is the fluctuation of N and n is the bulk density of defects. From this we conclude that the coercive field is proportional to $V^{1/2}/S$. For domain walls, VBL's and Bloch points we have $S_{DW} = dL$, $S_{VBL} \approx \delta d$, $S_{DW} \approx \delta^2$, and $V_{DW} = \delta dL$, $V_{VBL} \approx \delta^2 d$, $V_{DW} \approx \delta^3$ respectively. For $L = 10$ mm, $d = 100$ μm, $\delta = 0.2$ μm, we obtain the following ratios of the quantities H_c for the various microstructural elements: $H_c^{DW}:H_c^{VBL}:H_c^{BP} \approx 1:200:5000$, which agrees with the experimental results.

6. BLOCH POINTS IN AN AC MAGNETIC FIELD

Our investigations of Bloch-point oscillations in crossed magnetic fields show that during domain-wall oscillations excited by a field H_y the coercive field of a Bloch point decreases and its effective value ($\tilde{H}_c^{BP}$) depends on Δ_{DW}. An analogous decrease in the coercive field is also observed for the VBL. The value of $\tilde{H}_c^{BP}$ is determined using the function $\Delta_{BP}(H_x)$ for various values of Δ_{DW}. Figure 7 shows the function $H_{0x}(\Delta_{DW}) = \tilde{H}_c^{BP}(\Delta_{DW})$. The most rapid decrease in H_c^{BP} is observed for variations of Δ_{DW} within the interval 0 to 0.2 μm.

The observed effect can be explained in terms of the assumption made in the previous section that the clamping of a microstructural element is determined by fluctuations in the number of defects within the volume of the element. In this model the Bloch point is inseparably bound to a domain wall; when this domain wall oscillates with an amplitude $\sim\delta$ the coercivity of the Bloch point can be suppressed due to expulsion of the Bloch point moving along with the wall from a minimum of the potential contour for $\Delta_{DW} \sim \delta$; this initiates motion of the Bloch point along the y axis under the action of the field H_x. For small velocities of Bloch point motion as the latter migrates along the boundary in a field $H_x < H_c^{BP}$, an important role is apparently played by mechanisms analogous to those that cause creep of domain walls in thin magnetic films.[14] In this case the process of Bloch-point migration can be viewed as the result of a chain of microshifts of parts of the Bloch point mediated by the action of the pressure exerted by the field H_x and the activating influence of the domain wall oscillations. The quantity H_c^{BP} depends only weakly on f_y, the frequency of the field H_y, if f_y is greater than f_x, the frequency of oscillation of the Bloch point; apparently H_c^{BP} is primarily determined by the amplitude of the domain-wall oscillations.

Figure 7 may be viewed as a diagram in the coordinates (H_{0x}, Δ_{DW}) that characterizes the various dynamic behavior of the Bloch point. Region I located above the straight line $H_{0x}(\Delta_{DW}) = H_c^{BP}$ is the region of above-barrier motion

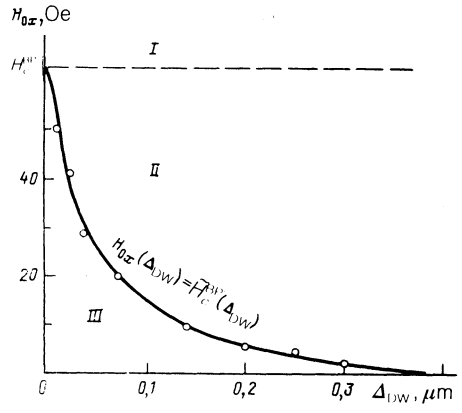

FIG. 7. Dependence of the effective coercive field of a Bloch point ($\tilde{H}_c^{BP}$) on the amplitude of domain wall oscillation; $f_x = 60$ Hz, $f_y = 44$ kHz. The letters I, II, III denote regions of various dynamic behavior of the Bloch point.

of the Bloch point. In region II motion of the Bloch point is possible only in the presence of domain-wall oscillations. Below the threshold curve $H_{0x}(\Delta_{DW}) = \tilde{H}_c^{BP}(\Delta_{DW})$, i.e., in region III, the Bloch point is at rest. In region II the spectrum of Bloch-point oscillations has a relaxational character as a function of the frequency f_x.

Examples of the relaxational spectra of $\Delta_{BP}(f_x)$ are shown in Fig. 8. It is clear that the relaxational frequency f_r of the Bloch point oscillation, defined as the frequency for which the function $\Delta_{BP}(f_x)$ reaches a value of 0.7 of its maximum value Δ_{BP}, depends both on the amplitude of the domain wall oscillation and on the magnitude of the field H_x. Small values of f_r correspond to those portions of region II that lie near the threshold of the curve; for regions increasingly distant from this curve f_r increases. By varying the parameters H_x and Δ_{DW} it is possible to obtain the spectrum down to $f_r \sim 10$ Hz.

For above-barrier motion ($H_x > H_c^{BP}$) the amplitude of Bloch point oscillations increases with frequency, with a considerable increase in Δ_{BP} for $f_x \gtrsim 100$ kHz. The cause of the observed effect is apparently a decrease in the coercive field H_c^{BP} connected with an increase of the velocity of the Bloch point as f_x increases. A falloff in the dynamic coercivity of a VBL as its velocity increases was predicted, e.g., by Popkov in Ref. 15. We can reasonably claim that an analogous decrease in the dynamic coercive field should also occur for a Bloch point.

7. CONCLUSIONS

We have carried out a detailed study of the near-surface substructure of 180° domain walls in filamentary iron single-crystals using a magneto-optic micromagnetometer. Our investigations have shown that as a whole the substructure has a regular character, i.e., the substructure has a period that depends on the crystal thickness. We have observed a regular order in the alternation of substructural elements: the domain-wall segments we observed most often were of type VBL-Bloch point-VBL, more rarely segments of type VBL–VBL. As a rule the Bloch point occupies an asymmetric position between two VBL's; this can be explained by the effect of stray fields arising from rather small deviations from parallelism of opposite facets of the crystals. On rare occasions we encounter groups of several Bloch points located between two VBL's.

The decreasing dimensionality of the microstructural elements in the domain wall, VBL, Bloch point sequence gives rise to an increase in H_c by one to three orders of magnitude. Demagnetization fields lead to a weakening of the magnetic field within the sample. The distribution of demagnetizing fields in samples that are not of ellipsoidal form is complicated. Inclusion of these fields leads to a decrease of H_c^{VBL} and H_c^{BP}. This decrease is roughly the same for both microstructural elements and does not change our general conclusions concerning the ratios of the coercive fields for a domain wall, a VBL, and a Bloch point.

In the presence of domain wall oscillations the values of the coercive fields of a Bloch point and a VBL decrease. The observed effect is naturally explained by the activating influence of domain wall oscillations on the motion of Bloch points and VBL's. This influence clearly can be viewed as expulsion of the Bloch point and VBL from minima in the potential contour caused by defects as the domain wall moves. This situation results in favorable conditions for shifting of Bloch points and VBL's in the presence of the fields H_x and H_z respectively. In the region $\tilde{H}_c^{BP} < H_x < H_c^{BP}$ the frequency dependence of the amplitude of Bloch point oscillations activated by domain wall oscillations has a relaxational form.

In the activated regime we have studied the process of Bloch-point and VBL motion for $\Delta_{DW} \sim \delta$ in a constant magnetic field. In this regime the Bloch point and VBL motions are opposite. The values of the coefficients K_x^{BP} and K_x^{VBL} which characterize the motion of microstructural elements in the fields H_x and H_z depend on the sample thickness and period of the substructure. The values of K_x^{BP} and

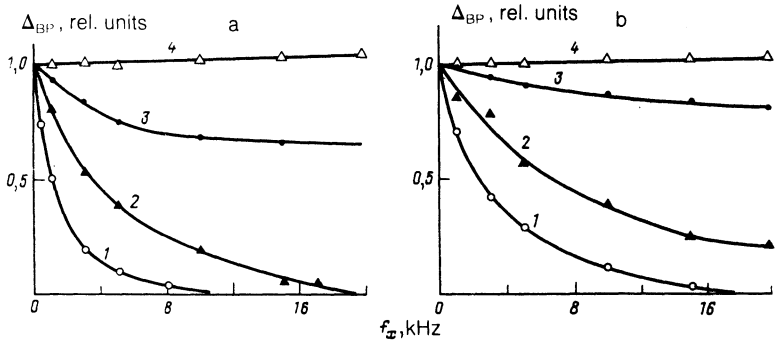

FIG. 8. Relaxational spectrum of Bloch point oscillation in a field H_x for one-dimensional domain-wall pumping at a frequency $f_y = 44$ kHz with amplitude 0.03 μm (a) and 0.1 μm (b). Curves *1* were measured in a field $H_x = 0.5 \cdot H_c^{BP}$, curves *2* in a field $H_x = 0.7 \cdot H_c^{BP}$, and curves *3* in a field $H_x = 0.9 \cdot H_c^{BP}$, where $H_c^{BP} = 55$ Oe. Curves *4* were measured in a field $H_x = 1.5 \cdot H_c^{BP}$ in the absence of domain-wall oscillations.

K_x^{VBL} determined by applying static and quasistatic fields coincide. We have also observed the process whereby Bloch points in pairs first approach and then annihilate one another as the field H_x increases.

[1] G. S. Krinchik and O. M. Benidze, Zh. Eksp. Teor. Fiz. **67**, 2180 (1974) [Sov. Phys. JETP **40**, 1081 (1974)].
[2] H. P. Oepen and J. Kirschner, J. Phys. **49**, 1853 (1988).
[3] A. Hubert, Z. angew. Phys. **32**, p. 58 (1971).
[4] V. E. Zubov, G. S. Krinchik, and A. D. Kudakov, Pis'ma Zh. Eksp. Teor. Fiz. **47**, 134 (1988) [JETP Lett. **47**, 161 (1988)]; Zh. Eksp. Teor. Fiz. **94**, 243 (1988) [Sov. Phys. JETP **67**, 2527 (1988)].
[5] S. S. Brenner, Acta Metall. **4**, 62 (1956).
[6] S. Shtrikman and J. Trevers, J. Appl. Phys. **31**, 1304 (1960).
[7] V. E. Zubov, G. S. Krinchik, and S. N. Kuz'menko, Pis'ma Zh. Eksp. Teor. Fiz. **51**, 419 (1990) [JETP Lett. **51**, 477 (1990)].
[8] A. P. Malozemoff and J. C. Slonczewski *Magnetic Domain Walls in Bubble Materials*, Academic, New York, (1979).
[9] G. V. Berezhkova, *Filamentary Single Crystals*, Nauka, Moscow, 1969.
[10] I. P. Kushnir, Kristallografiya **12**, 474 (1967) [Sov. Phys. Crystallogr. **12**, 405 (1967)].
[11] B. Heinrich, K. B. Urguhart, S. T. Dutcher *et al.*, J. Appl. Phys. **63**, 3863 (1988).
[12] J. Millat, V. Laska, A. Thiaville, and F. Boileau, J. Phys. **49**, 1871 (1988).
[13] L. J. Dijkstra and C. Wert, Phys. Rev. **79**, 979 (1950).
[14] R. V. Telesnin, O. A. Vinogradov, E. N. Pl'icheva *et al.*, *Physics of Metal Films*, p. 15 [in Russian]. Nauk, Dumka, Kiev, 1968. E. N. Pl'icheva, R. Liu-Fa-Chun *et al.*, *Abstracts from the Intl. Symp. on the Physics of Magnetic Films*, p. 226 [in Russian], Irkutsk, 1968.
[15] A. F. Popkov, Zh. Eksp. Teor. Fiz. **97**, 965 (1990) [Sov. Phys. JETP **70**, 541 (1990)].

Translated by Frank J. Crowne